SCIENCE CHINA
Information Sciences

September 2020, Vol. 63 190201:1–190201:16
https://doi.org/10.1007/s11432-019-2987-x

• RESEARCH PAPER •
Special Focus on Driver Automation Collaboration and Augmentation in Automated Driving

Driver-automation shared steering control for highly automated vehicles

Jun LIU[1,2], Hongyan GUO[1,2*], Linhuan SONG[4], Qikun DAI[2] & Hong CHEN[3,2]

[1]*State Key Laboratory of Automotive Simulation and Control, Jilin University, Changchun* 130022*, China;*
[2]*College of Communication Engineering, Jilin University, Changchun* 130022*, China;*
[3]*Clean Energy Automotive Engineering Center, Tongji University, Shanghai* 201804*, China;*
[4]*Intelligent Connected Vehicle Development Institute, China Faw Corporation Limited, Changchun* 130011*, China*

Received 17 October 2019/Revised 26 May 2020/Accepted 9 July 2020/Published online 12 August 2020

Abstract A model predictive control (MPC)-based shared steering framework for intelligent vehicles is proposed in this paper. The road boundary and vehicle stability boundary are regarded as the safe envelope, and the tradeoff between the freedom of driver operation and safety assurance of intelligent vehicles is made within this safe envelope. Under this cooperative steering framework, the reliability of drivers is analyzed in dangerous situations and in the predictive time domain, and two improved schemes are proposed. Under the two improved schemes, the weight of the control objective can be adaptively changed according to the results of the threat assessment and predetermined strategy. At the same time, an evaluation index named control intervention rate and risk rate is proposed to evaluate the designed human-vehicle cooperation scheme. The simulation results show that the performance of the two improved schemes in ensuring the safety of intelligent vehicles has been improved.

Keywords shared steering control, moving horizon optimization, hazard evaluation, intelligent vehicle, safe envelope

Citation Liu J, Guo H Y, Song L H, et al. Driver-automation shared steering control for highly automated vehicles. Sci China Inf Sci, 2020, 63(9): 190201, https://doi.org/10.1007/s11432-019-2987-x

1 Introduction

Automated driving technology has been widely promoted in perception, decision-making and control, and enterprise-led real vehicle projects [1, 2]. Developed countries and some manufacturers have also formulated plans to develop fully automated vehicles and have pioneered automated driving systems, highlighting their important role in reducing road traffic accidents [3, 4]. Even traditional car manufacturers such as BMW, Mercedes, and Audi have launched similar automated driving systems [5]. However, the average number of accidents of autonomous vehicles is higher than that of traditional vehicles with the current level of technology [6], which causes most drivers to be concerned about the safety of autonomous vehicles [7]. Thus, the large-scale application of fully automated vehicles requires a long transition stage, that is, the cooperation of manual driving and automated driving will exist for a long time. Coordinating the relationship between drivers and automated driving systems introduces new academic and technological challenges.

Considering the significant potential for avoiding collisions through steering operation, many scholars have conducted research on cooperative steering control [8]. Cooperative steering initially appeared in the form of torque assistance, which is also called haptic shared control because the moment interacts

* Corresponding author (email: guohy11@jlu.edu.cn)

with the neuromuscular force of the driver's arm through the steering wheel [9]. Electric power steering (EPS), a classical haptic shared control, assists drivers in completing the steering operation by applying additional moments to improve the steering portability of the vehicle [10]. The key factor in haptic shared control is determining the desired assistant moment that meets the human neuromuscular motion characteristics [11,12]. Abbink et al. [13] noted that if torque assistance does not match the neuromuscular behavior of human drivers, then the performance of haptic shared control will be greatly reduced. Aiming to solve the matching problem between moment assistance and driver neuromuscular characteristics, Iwano et al. [14] explored a cooperative relationship between the driver and active steering system in reconstructed dangerous scenes. Occasional conflicts between nonpersonalized shared control systems and personalized human drivers can lead to performance degradation or even deterioration [15]. Moreover, the parameters of the haptic shared controller must be adjusted according to changes in the road environment and the driver's muscle states [11].

Steering-by-wire technology disconnects the steering wheel from the front wheels, which makes it possible for the controller to modify the driver's command at the actuator level [16]. Correspondingly, a shared steering mode called parallel steering control has emerged, in which the final front wheel angle is a blending of the human driver and automation. Some scholars hold the opinion that the share of driving between human and machine should be adjusted adaptively according to the driver's intention [17, 18]. In [19], a risk assessment decision-making strategy is proposed to determine the share of driving between human and machine, in which the vehicle longitudinal speed variation is regarded as the primary factor. Petermeijer et al. [20] designed a shared control logic to assist drivers only when necessary to guarantee the driver's freedom, in which the path is described by homotopy theory. However, an intention conflict inevitably still appears between the human driver and automation in the parallel mode. Na et al. [21] utilized game theory to explore the behavior evolution of the human driver and automation in the cooperative mode and noncooperative state.

In contrast to parallel control, envelope control can allow drivers to operate intelligent vehicles freely within safe limits [22]. The successful application of this approach in the aircraft industry has proven that envelope control is a potential shared control method for intelligent vehicles, and it can also alleviate driver discomfort caused by conflicts between human drivers and automation. Switkes et al. [19] proposed an envelope control system based on steering-by-wire technology to ensure the stability of the vehicle, and this system only corrects the front wheel angle of the driver at the actuator level when necessary. When the tire reaches the nonlinear zone, it will introduce great challenges for stability control. Erlien et al. [23] regarded the nonlinear characteristics of tires as an indispensable key factor when modeling for shared steering control. The system can accurately intervene to ensure vehicle safety if the tires reach the nonlinear zone. Similar to this system, a two-envelope control method was proposed to protect the vehicles from collisions, in which the steering angle bound and road boundary were regarded for the safe envelope [24].

As a typical man-machine system, driver-automation system can achieve better overall performance with a deep understanding of the driver's characteristics. However, if real human driver is used to design, test and evaluate the shared steering system, it is obviously time-consuming and expensive, and even dangerous. Therefore, it is the first choice for researchers to establish a driver model which can reflect the driver's characteristics instead of real human driver. For haptic shared control, the two-point preview driver model is the most commonly used driver model, which can realize the moment interaction between driver and automation [25, 26]. As for the parallel control mode, most scholars use the driver model based on model predictive control (MPC) to express the interaction relationship between human and automation by changing its internal model [21,27]. Different from parallel control mode, envelope control is to improve the vehicle safety by correcting driver's misoperation. It has higher tolerance to the form of driver's model, as long as it can reflect the required driver's characteristics, such as single-point preview and MPC-based driver model [28]. It is also one of the advantages of envelope control that the driver's characteristics do not need to be paid too much attention to. It is worth mentioning that the driver-automation system may also reshape the driver's characteristics, and there is a lack of research in this aspect at present [29].

The emergence of a driver-vehicle cooperative system has made the original independent driver and vehicle become a driver-vehicle coupled system. In contrast to traditional vehicle testing and evaluation, the object of testing and evaluation has changed from an independent vehicle system to a driver-vehicle strongly coupled system [30]. Test scenarios and tasks need to be redesigned to demonstrate the effectiveness and reliability of the functions and modules of the driver-vehicle system. Considering the ability of task completion, path tracking performance has been proposed to evaluate the driver-vehicle cooperative system [31,32]. From the perspective of safety, the minimum time of collision was calculated to measure driver-vehicle cooperative system performance [20]. To ensure comfort, Saleh et al. [33] proposed a consistency index of driver and automation operations to test the cooperative system. Moreover, Wang et al. [34] suggested that the man-machine collaboration system should be evaluated from the perspective of reducing driver workload. Although many scholars have presented their own opinions, the evaluation of the man-machine system is still in the exploratory stage.

This paper proposes an envelope control method to address the shared steering relationship between human drivers and controllers. The advantage of this scheme is that the operation freedom of the driver can be expanded as far as possible while the driver still remains in the loop. But relatively late intervention time and sudden intervention limit the performance of the origin scheme in ensuring vehicle safety. In order to improve defects of the original scheme, two improved methods based on hazard analysis and variable weight objective function in predictive horizon are proposed. One improved method is to establish the relationship between the objective function weight and hazard risk analysis result by using fuzzy logic. The other improved method is to change authority between the human driver and lane-keeping objective according to the reliability of the driver in the predictive time domain. Moreover, two novel indexes based on statistical theory are proposed to make up for the lack of quantitative evaluation indexes of shared steering system. Various simulation experiments are carried out to compare the comprehensive performance of the three shared steering schemes, and the simulation results prove that two improved schemes can both reduce the vehicle state oscillation and enhance the safety of intelligent vehicles.

The remainder of this paper is organized as follows. In Section 2, the shared steering framework is presented. Then, the shared steering control strategy design and the improved schemes are shown in Sections 3 and 4. Section 5 presents the performance index, and Section 6 shows the simulation results and evaluations. Section 7 provides a brief conclusion to the paper.

2 Model and problem description

2.1 Vehicle modeling

The lateral motion of a vehicle is mainly controlled by steering, and the corresponding major advantage of shared steering control is to assist the driver in manipulating the lateral motion of the vehicle. Therefore, it is necessary to establish a vehicle model that is capable of describing the vehicle position and lateral dynamics for a shared steering controller.

In this subsection, a classical bicycle dynamic model is established, as shown in Figure 1, which has been proven to be able to accurately describe vehicle dynamics when the tire works with a linear characteristic [35]. XOY is an inertial coordinate system, and xCoGy is the vehicle body-fixed coordinate system, whose origin is defined as the center of gravity (CoG). The x-axis in Figure 1 is pointing in the forward direction of the vehicle, and the x-axis rotates 90 degrees counterclockwise to obtain the y-axis. The directions of the z-axis are accordingly determined by the right-hand rule. The lateral position, yaw angle, sideslip angle and yaw rate are the selected states for describing the lateral kinematics and dynamics of the intelligent vehicle. Integrating the deduction in [36,37], the state-space description is shown as follows:

$$\dot{x} = Ax + B\delta_f, \tag{1a}$$

$$y = Cx, \tag{1b}$$

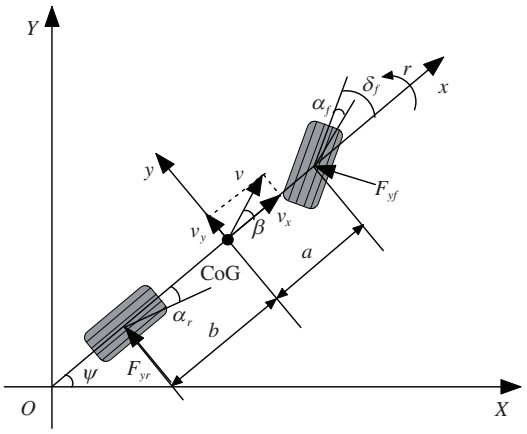

Figure 1 A 2-DOF vehicle model.

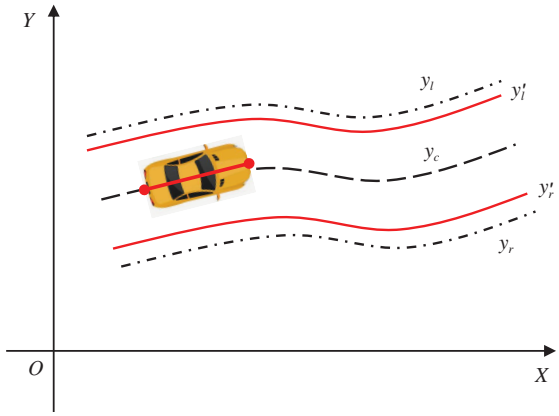

Figure 2 (Color online) Schematic diagram of the intelligent vehicle shared steering control.

where $x = [y_o \ \psi \ \beta \ r]$ is the vehicle. y_o is the lateral displacement, ψ is the yaw angle, β represents the sideslip angle, and r represents the yaw rate. $y = y_o$ is defined as the model output, and δ_f is the front wheel steering angle defined as the model input. The matrices in the above equation are as follows:

$$A = \begin{bmatrix} 0 & v & v & 0 \\ 0 & 0 & 0 & 1 \\ 0 & 0 & \dfrac{C_f + C_r}{mv} & \dfrac{aC_f - bC_r}{mv^2} - 1 \\ 0 & 0 & \dfrac{aC_f - bC_r}{I_z} & \dfrac{a^2C_f + b^2C_r}{I_z v} \end{bmatrix}, \quad B = \begin{bmatrix} 0 \\ 0 \\ -\dfrac{C_f}{mv} \\ -\dfrac{aC_f}{I_z} \end{bmatrix}, \quad C = \begin{bmatrix} 1 \\ 0 \\ 0 \\ 0 \end{bmatrix}^{\mathrm{T}},$$

where v is the vehicle longitudinal velocity, m represents the vehicle mass, and I_z denotes the moment of inertia. a and b in the above matrices represent the distances from the CoG to the front and rear axles, respectively. C_f and C_r denote the front and rear tire cornering stiffnesses, respectively. Note that it is necessary to transform Eq. (1) into a discrete form for controller design:

$$\begin{aligned} x(k+1) &= A_c x(k) + B_c \delta_f(k), \\ y(k) &= C_c x(k), \end{aligned} \tag{2}$$

where $A_c = e^{AT_s}$, $B_c = \int_0^{T_s} e^{A\tau} \mathrm{d}\tau \cdot B$, $C_c = C$, and T_s is the sampling time.

2.2 Problem description

Shared steering control of an intelligent vehicle means that an intelligent vehicle will be operated by a human driver and a shared steering controller. The control problem can be described as ensuring that the vehicle runs in the feasible area by designing a controller to coordinate the driver's steering operation. The specific feature is that the steering operation by the human driver is fully executed by the vehicle when the vehicle operates in a feasible road region. The shared steering control system corrects the driver's steering operation only if a collision or instability is about to occur.

For the aforementioned feature, the shared steering control can be transformed into a problem that confines the vehicle lateral displacement in a feasible road region. The feasible road region can be considered as the inner area of the lane contained in the lane boundary. In Figure 2, the left and right boundaries of the road are represented by y_l and y_r, respectively, and y_c represents the centerline of the road. However, it is not sufficient to confine the center of mass of the vehicle to the feasible area, and the geometric shape of the vehicle should also be considered. Therefore, the geometric shape of the intelligent vehicle can be reduced to a rigid bar with a length of l, and the feasible area also needs to be reduced by half the width of the vehicle inward. If the front and rear of the simplified rigid bar are confined to the feasible area, the vehicle will not collide with the road boundary.

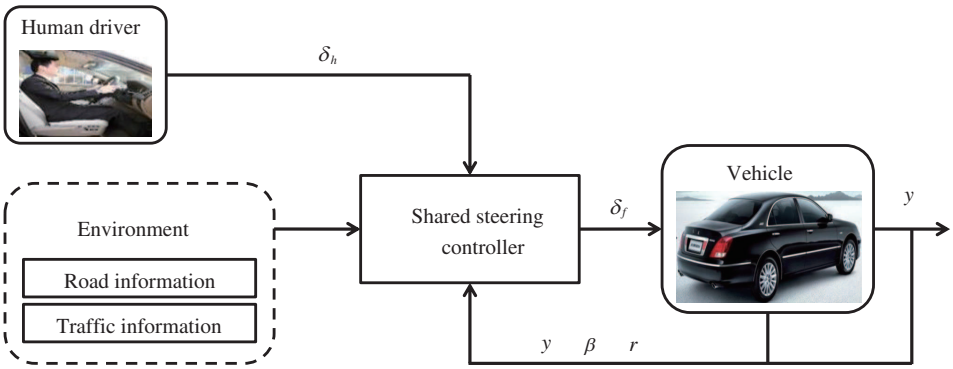

Figure 3 (Color online) Control block diagram of the shared steering vehicle.

3 Structure and control strategy design

3.1 Shared steering envelope control structure

The shared steering envelope control structure shown in Figure 3 assists drivers in completing steering tasks to reduce the risk of collisions. As mentioned in Subsection 2.2, shared steering envelope control not only follows the driver's intention, but also needs to corrects the driver's steering operation if a collision or instability is about to occur. Moreover, vehicle states also needs to meet the dynamic and kinematic constraints. All these characteristics make shared steering envelope control a standard optimization problem with constraints, and MPC has been widely used in dealing with optimization problem with constraints because of its inherent predictive and constraint handling capabilities [38, 39]. First, the road boundary and vehicle stability boundary, regarded as an envelope, act as constraints for shared steering envelope control problems. The driver's actions are collected as a reference to follow the driver's intention as far as possible under the condition of ensuring vehicle safety. The traffic and road environment information is assumed to be known information obtained from the sensor module. The optimization problem is calculated at each step to provide the necessary steering intervention that protects intelligent vehicles from instability and collisions.

3.2 Shared steering envelope control strategy

In this subsection, an MPC-based shared steering strategy using an envelope strategy is designed to provide steering assistance for human drivers. Eq. (2) acts as a predictive model, and the predicted state and output of the system are defined as follows:

$$\begin{aligned} X(k+1|k) &\triangleq S_{xx}x(k) + S_{xu}U(k), \\ Y(k+1|k) &\triangleq S_x x(k) + S_u U(k). \end{aligned} \tag{3}$$

The concrete expressions of the matrix variables in Eq. (3) are as follows:

$$S_{xu} = \begin{bmatrix} B_c & 0 & \cdots & 0 \\ \vdots & \vdots & & \vdots \\ A_c^{N-1}B_c & A_c^{N-2}B_c & \cdots & B_c \\ \vdots & \vdots & & \vdots \\ A_c^{P-1}B_c & A_c^{P-2}B_c & \cdots & \sum_{i=1}^{P-N+1} A_c^i B_c \end{bmatrix}, \quad S_u = \begin{bmatrix} C_c B_c & 0 & \cdots & 0 \\ \vdots & \vdots & & \vdots \\ C_c A_c^{N-1}B_c & C_c A_c^{N-2}B_c & \cdots & C_c B_c \\ \vdots & \vdots & & \vdots \\ C_c A_c^{P-1}B_c & C_c A_c^{P-2}B_c & \cdots & \sum_{i=1}^{P-N+1} C_c A_c^i B_c \end{bmatrix},$$

$$S_x=\begin{bmatrix} C_dA_d \\ \vdots \\ C_dA_d^N \\ \vdots \\ C_dA_d^P \end{bmatrix},\ S_{xx}=\begin{bmatrix} A_c \\ \vdots \\ A_c^N \\ \vdots \\ A_c^P \end{bmatrix},\ U(k)=\begin{bmatrix} \delta_f(k|k) \\ \delta_f(k+1|k) \\ \vdots \\ \delta_f(k+P-1|k) \end{bmatrix},\ X(k)=\begin{bmatrix} x(k+1|k) \\ x(k+2|k) \\ \vdots \\ x(k+P|k) \end{bmatrix},\ Y(k)=\begin{bmatrix} y(k+1|k) \\ y(k+2|k) \\ \vdots \\ y(k+P|k) \end{bmatrix},$$

where the symbols N and P represent the control time domain and predictive time domain, respectively, with $P \geqslant N$, and the control variables remain unchanged in the predicted time domain when the control time domain is exceeded, that is, $\delta_f(k+N-1)=\delta_f(k+N)=\cdots=\delta_f(k+P-1)$.

In the proposed shared control framework, it is a core feature to following the driver's characteristics and driving intention. The driver's characteristics and intention are generally reflected in the driver's operation. Since following the driver's intention is considered to be an important objective in shared steering envelope controller design, it can be realized by minimizing the following objective function:

$$J_1 = |U_h(k) - U(k)|, \tag{4}$$

where $U_h(k) = [\delta_h(k|k)\ \delta_h(k+1|k)\ \cdots\ \delta_h(k+P-1|k)]^{\mathrm{T}}$. The driver's steering operation in the predictive horizon remains unchanged, that is, $\delta_h(k|k)=\delta_h(k+1|k)=\cdots=\delta_h(k+P-1|k)$.

Considering that excessive control action will make the state of the vehicle system dramatically change, which will increase the driver's discomfort, it is necessary to ensure that the control action changes as smoothly as possible:

$$J_2 = \sum_{i=1}^{P-1}(\delta_f(k+i) - \delta_f(k+i-1))^2. \tag{5}$$

Since two control objectives cannot be minimized simultaneously, a weighting factor Γ_δ is introduced as a tradeoff between safety and comfort. This kind of transformation can weaken the conflicts between different performance requirements, and the corresponding objective function is finally transformed into the following form:

$$J_H = J_1 + \Gamma_\delta J_2. \tag{6}$$

The safe envelope is mainly composed of two parts: the kinematics envelope and the dynamics envelope. The kinematics envelope describes the range of the feasible driving area, which can ensure that the vehicle does not collide in this area. It can be expressed in terms of inequalities as follows:

$$C_r x(k+i) \leqslant b_r, \tag{7}$$

where

$$C_r = \begin{bmatrix} 1 & l_f & l_f & 0 \\ -1 & -l_r & -l_r & 0 \\ 1 & -l_r & -l_r & 0 \\ -1 & l_r & l_r & 0 \end{bmatrix},\quad b_r = \begin{bmatrix} y_l - \dfrac{w}{2} - \omega_p \\ -y_r - \dfrac{w}{2} - \omega_p \\ y_l - \dfrac{w}{2} - \omega_p \\ -y_r - \dfrac{w}{2} - \omega_p \end{bmatrix}.$$

The dynamics envelope represents the variable range of vehicle states, which can be expressed by the following inequality:

$$C_s x(k+i) \leqslant b_s, \tag{8}$$

where

$$C_s = \begin{bmatrix} 0 & 0 & 0 & 1 \\ 0 & 0 & 1 & -\dfrac{b}{v_x} \\ 0 & 0 & 0 & -1 \\ 0 & 0 & -1 & -\dfrac{b}{v_x} \end{bmatrix},\quad b_s = \begin{bmatrix} \dfrac{g\mu}{v_x} \\ \alpha_{r,\mathrm{sat}} \\ \dfrac{g\mu}{v_x} \\ \alpha_{r,\mathrm{sat}} \end{bmatrix}.$$

The saturation of the mechanical system should be taken into consideration when designing the control strategy, and the steering constraints are formulated as follows:

$$|\delta_f(k+i)| \leqslant \delta_{f,\mathrm{sat}}, \tag{9}$$

where $\delta_f(k+i)$ is the front wheel angle at step $k+i$ and $\delta_{f,\mathrm{sat}}$ is the maximum allowable front wheel angle of the steering system.

Moreover, the smoothness of control actions can be guaranteed by limiting the variation between two-step control actions:

$$|\Delta\delta_f(k+i)| \leqslant \dot{\delta}_{f,\mathrm{sat}} T_s. \tag{10}$$

Finally, the shared steering envelope control strategy is transformed into a constrained optimization problem, and this control strategy, denoted by NO AUTO, is expressed as

$$\min_{U(k)} J_{\mathrm{scheme1}} = J_H, \tag{11a}$$

$$\text{s.t. } C_r x(k+i) \leqslant b_r, \tag{11b}$$

$$C_s x(k+i) \leqslant b_s, \tag{11c}$$

$$i = 1, 2, \ldots, p, \tag{11d}$$

$$|\delta_f(k+j)| \leqslant \delta_{f,\mathrm{sat}}, \tag{11e}$$

$$|\Delta\delta_f(k+j)| \leqslant \dot{\delta}_{f,\mathrm{sat}} T_s, \tag{11f}$$

$$j = 1, 2, \ldots, m. \tag{11g}$$

4 Improved driver-automation collaboration schemes

The working mode of the controller designed in Section 3 is to ensure the safety of the vehicle by correcting the driver's misoperation. There is a transition process from safe states to dangerous states, and the controller only intervenes in vehicle control when the process is near the end, which limits the performance of the controller in ensuring vehicle safety. Moreover, the sudden intervention of the controller may lead to the conflict between the driver and the controller when the vehicle is about to be in danger, thus increasing the risk of the vehicle safety. Considering the above defects, two improved schemes are proposed to enhance the performance of the controller. On the one hand, the intervention time of the controller is advanced to strengthen the controller ability in ensuring vehicle safety. On the other hand, the intervention process of the controller is designed to be smoother to reduce the risk caused by driver-controller conflict.

4.1 Hazard-evaluation-based shared steering envelope control

If the controller only intervenes in the case of imminent collision or instability, it is likely to cause drastic changes in the vehicle system states. Therefore, it is necessary for the controller to cooperate with the driver to participate in the steering control of the vehicle in advance before the danger occurs. Therefore, an additional objective of the controller must be designed as follows:

$$J_A = \Gamma_y \|Y(k) - Y_c(k)\| + \Gamma_\beta \sum_{i=1}^{p} \left(\beta(k+i)\right)^2, \tag{12}$$

where $Y_c(k)$ is the road centerline assumed as the desired path. Moreover, $\Gamma_y = \mathrm{diag}(\Gamma_{y,1}, \Gamma_{y,2}, \ldots, \Gamma_{y,p})$ and $\Gamma_\beta = \mathrm{diag}(\Gamma_{\beta,1}, \Gamma_{\beta,2}, \ldots, \Gamma_{\beta,p})$ are the weight matrices.

The additional objective Eq. (12) cannot only assist the driver in driving along the desired trajectory but also avoid the instability caused by the large sideslip angle. Combining the objective J_H and the additional objective J_A, we finally obtain the following improved objective:

$$J(y(k), U(k), m, p) = J_H + \Gamma J_A, \tag{13}$$

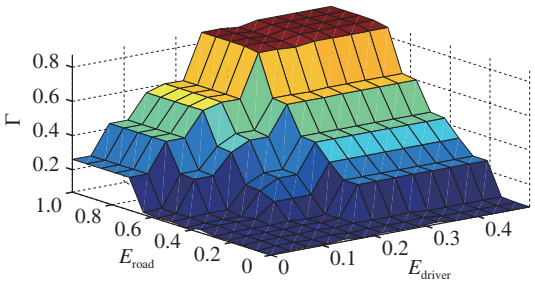

Figure 4 (Color online) Hazard evaluation map.

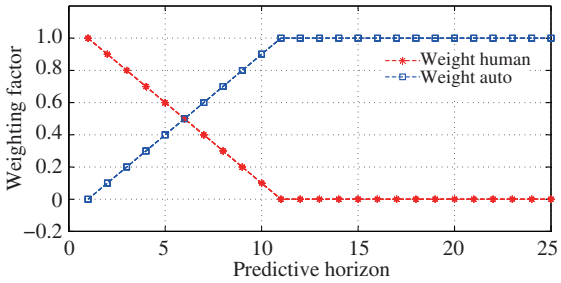

Figure 5 (Color online) Objective weights in predictive horizon.

where Γ is the weight matrix. As concluded from Eq. (13), the design of weighting factor Γ matters if the shared steering envelope controller wants to achieve the desired performance. Therefore, the weighting factor is designed by a hazard evaluation module, in which collision risk and driver failure risk are taken into consideration.

Collision risk means the possibility of a collision of an intelligent vehicle, defined as follows:

$$E_{\text{road}} = |y(k) - y_c(k)|^{E_A}, \tag{14}$$

where $|y(k) - y_c(k)|$ is the vehicle lateral position deviation and $E_A > 0$ is a positive constant.

In addition, the driver failure risk describes the degree of deviation between the driver's current operation and the desired operation at the current moment, and the index is expressed as follows:

$$E_{\text{driver}} = \frac{|\delta_{\text{human}}(k) - \delta_f(k|k-1)|}{E_B}, \tag{15}$$

where E_B is a regulating variable that makes E_{road} and E_{driver} of the same order of magnitude, and $\delta(k|k-1)$ is the step k desired steering operation optimized at step $k-1$.

Fuzzy logic is used to establish the relationship between the weighting factor Γ and the hazard evaluation module, collision risk E_{road} and driver failure risk E_{driver}. After adjustment, a three-dimensional map of weight factor Γ is obtained, as shown in Figure 4, and the weighting factor can be obtained by looking up a map if the collision risk and driver failure risk are calculated.

This improved strategy is named hazard-evaluation-based shared steering envelope control, denoted by FUZZY, and it can be defined as follows:

$$\min_{U(k)} J_{\text{scheme2}} = J_H + \Gamma J_A \tag{16a}$$

$$\text{s.t. } C_r x(k+i) \leqslant b_r, \tag{16b}$$

$$C_s x(k+i) \leqslant b_s, \tag{16c}$$

$$i = 1, 2, \ldots, p, \tag{16d}$$

$$|\delta_f(k+j)| \leqslant \delta_{f,\text{sat}}, \tag{16e}$$

$$|\Delta\delta_f(k+j)| \leqslant \dot{\delta}_{f,\text{sat}} T_s, \tag{16f}$$

$$j = 1, 2, \ldots, m. \tag{16g}$$

4.2 Take-over-based shared steering control

The take-over-based shared steering control does not focus on following the driver steering operation in the predictive horizon. The authority transform of the shared steering optimization objective is added to the scheme. Because of the introduction of the new control objectives, new rules of weight change are designed to balance the role of the two objectives:

$$J_{\text{scheme3}} = \omega(i) J_1 + (1 - \omega(i)) J_A. \tag{17}$$

In this paper, the transform rule $\omega(i)$ is described by the piecewise function shown in Figure 5. The

line called weight human is the changing rule of J_1 in the predictive horizon, and the line called weight auto is the changing rule of J_A in the predictive horizon.

This take-over-based shared steering control scheme is represented by the abbreviation horizon, and its optimization problem can be described as follows:

$$\min_{U(k)} J_{\text{scheme3}} = \omega(i)J_1 + (1-\omega(i))J_A \tag{18a}$$

$$\text{s.t. } C_r x(k+i) \leqslant b_r, \tag{18b}$$

$$C_s x(k+i) \leqslant b_s, \tag{18c}$$

$$i = 1, 2, \ldots, p, \tag{18d}$$

$$|\delta_f(k+j)| \leqslant \delta_{f,\text{sat}}, \tag{18e}$$

$$|\Delta\delta_f(k+j)| \leqslant \dot{\delta}_{f,\text{sat}} T_s, \tag{18f}$$

$$j = 1, 2, \ldots, m. \tag{18g}$$

5 Metrics to evaluate performance

The evaluation of shared steering envelope control performance generally considers the tradeoff among multiple evaluation indexes. The main purpose of a shared steering envelope control system is that it can help drivers keep vehicles out of collisions and improve active safety. At the same time, envelope control is characterized by not interfering with the driver's operation to the greatest extent possible when there is no danger. In the absence of systematic evaluation criteria, we define two statistical-based evaluation indexes to evaluate the performance of shared steering envelope control systems.

One of the most common vehicle safety evaluation indexes is whether a vehicle collides with another vehicle or road boundary. However, there are many reasons for vehicle collision accidents, and it is almost impossible to find a unified logic to analyze the performance of driver assistance systems. Therefore, to overcome this difficulty, we propose a probability description index based on statistics to describe the risk probability of vehicles from a macro perspective in the running process. This index, called hazard rate, is the ratio of vehicle running time beyond the road boundary to the total vehicle running time, which can be expressed in the following form.

$$\textbf{Hazard rate:} \quad \frac{T_{E_{r,\text{threshold}}}}{T_{\text{total}}} \times 100\%, \tag{19}$$

where $T_{E_{r,\text{threshold}}}$ represents the time length when the vehicle collides with or is beyond the road boundary and T_{total} is the total time length of vehicle operation.

In the framework of shared steering envelope control, drivers are allowed to operate the vehicle freely unless the vehicle is about to reach or exceeded the envelope. However, if the system is too sensitive and intervenes frequently, drivers will feel annoyed, and their subjective evaluation of the shared steering envelope control system will be reduced. Therefore, an index called control intervention rate is proposed, which expresses the average intervention level of the system to driver operation over a period of time. And the specific form of this index is shown in Eq. (20). The higher the system intervention frequency and the larger the correction control action amplitude, the higher the index, or vice versa. This index is zero when the system does not intervene in the driver's operation completely.

$$\textbf{Control intervention rate:} \quad \frac{\int (\frac{|\delta_h - \delta_f|}{\delta_{f,\max}}) \mathrm{d}t}{T_{\text{total}}} \times 100\%, \tag{20}$$

where δ_h represents the front wheel steering angle that the driver expected and δ_f represents the front

Table 1 Driver types and characteristics

Driver type	Driver characteristics
D1	skillful, careful, smooth with preview
D2	skillful, racy, direct with preview
D3	without preview
D4	untrained, racy, direct with preview

wheel steering angle of the controller output. $\delta_{f,\max}$ represents the maximum front wheel angle provided by the system. T_{total} represents the total time to indicate the working condition.

6 Results and discussion

To verify the effect of the above shared steering control scheme, double-lane change and slalom driving tasks in low- and high-risk simulation scenarios were performed in the virtual environment of the veDYNA software platform. Since different drivers also have various driving skills, a driver model with specific driving skills established in the veDYNA platform was used in the simulation experiment to represent various types of drivers. The classification and characteristics of the drivers are shown in Table 1. The simulation results and analysis of three shared steering control schemes are shown below.

6.1 Simulation results in low-risk scenarios

As mentioned above, the shared steering envelope control, the hazard-evaluation-based shared steering control and take-over-based shared steering control are marked as NO AUTO, FUZZY, and HORIZON, respectively. We first validate the proposed framework in low-risk scenarios, and the vehicle speed and road friction coefficient were set to 50 km/h and 0.85, respectively. All four types of drivers shown in Table 1 were selected to perform the driving task, in which the driving test road is shown in the first picture of Figure 6(a). Several studies [40, 41] have found that drivers do not always drive along the centerline of the road, and the desired path was a 0.2 m deviation from the centerline to represent that the driver was not always required to follow the centerline. More detailed evaluation results are shown in Figure 7.

In the low-risk lane-change scenario, the type D1 driver was selected to perform the driving task. The vehicle was running in the drivable area of the road, the vehicle states were all in a stable range, and the driver played a leading role in shared steering conditions. Because the desired path was a 0.2 m deviation from the centerline and the weight assigned to the objective of tracking the centerline in the HORIZON scheme became heavier, vehicles were more restricted to tracking the centerline of the road, which can be verified by the fact that the red dotted line is closer to the centerline. The control intervention rates of the three schemes were 0.0950%, 0.0945%, and 0.9414%, and these results also show that the HORIZON scheme tends to interfere with drivers following the centerlines, although the vehicle is in safer states. However, these characteristic differences can be neglected because the vehicle state curves of the three schemes in Figure 6 almost coincide with each other in low-risk scenarios.

Considering the relatively low hazard rate index in low-risk scenarios, only the intervention rate index is discussed here. The average intervention rates of the three schemes when faced with different types of drivers are shown in Table 2. Once the vehicle drives off the centerline, the controller of the HORIZON scheme will intervene more frequently to correct the driver following the centerline, which leads to a relatively higher average intervention rate. Because D1 and D2 types of drivers have better driving skills, drivers can rely on their own ability to control vehicles in safe areas most of the time, resulting in a lower intervention rate. In contrast, types D3 and D4 drivers need a relatively higher driving intervention rate because of their poor driving skills, as shown in Figure 7.

6.2 Simulation results in high-risk scenarios

To further verify the performance of the three shared steering schemes in high-risk scenarios, this paper

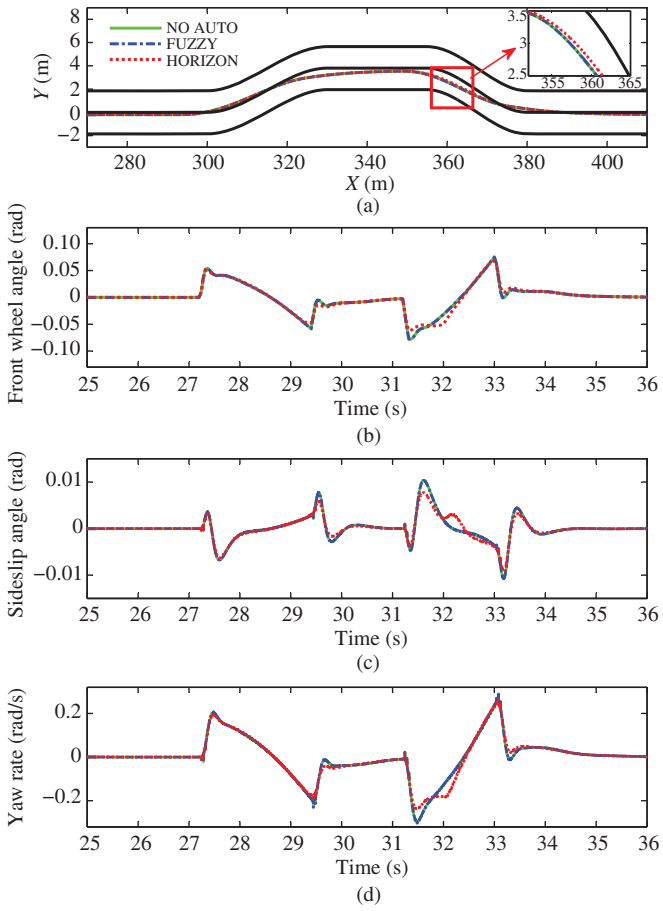

Figure 6 Simulation results of low-risk lane change. (a) Vehicle trajectory; (b) front wheel angle; (c) sideslip angle; (d) yaw rate.

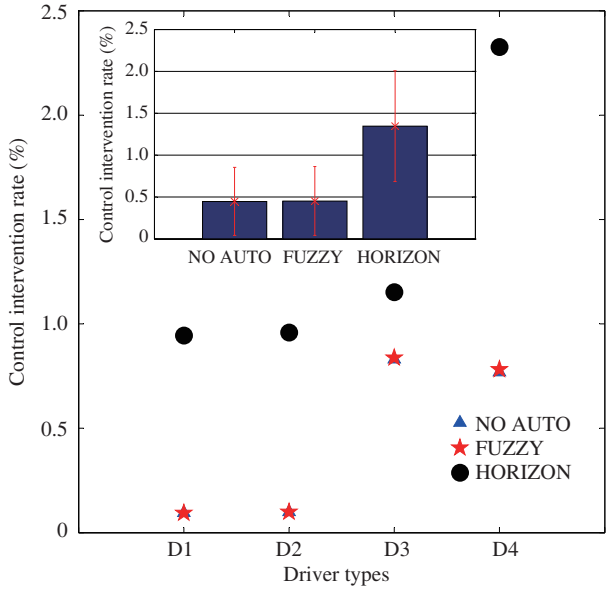

Figure 7 Comparison of low-risk lane change test results.

performed different high-risk virtual tests on the veDYNA platform, as presented in Table 3. The simulation results of tests 2 and 4 are presented in detail in Figures 8 and 9. Other simulation results are

Table 2 Performance of three schemes in low-risk scenarios

Index	NO AUTO	FUZZY	HORIZON
Average intervention rate (%)	0.4482	0.4531	1.3453

Table 3 High-risk virtual tests

No.	Test scenario	Driver type	Velocity (km/h)	Friction coefficient
1	slalom	D1	80	0.75
2	double-lane change	D1	100	0.55
3	obstacle avoidance	D1	50	0.55
4	slalom	D2	85	0.75
5	double-lane change	D4	85	0.55
6	double-lane change	D3	75	0.55

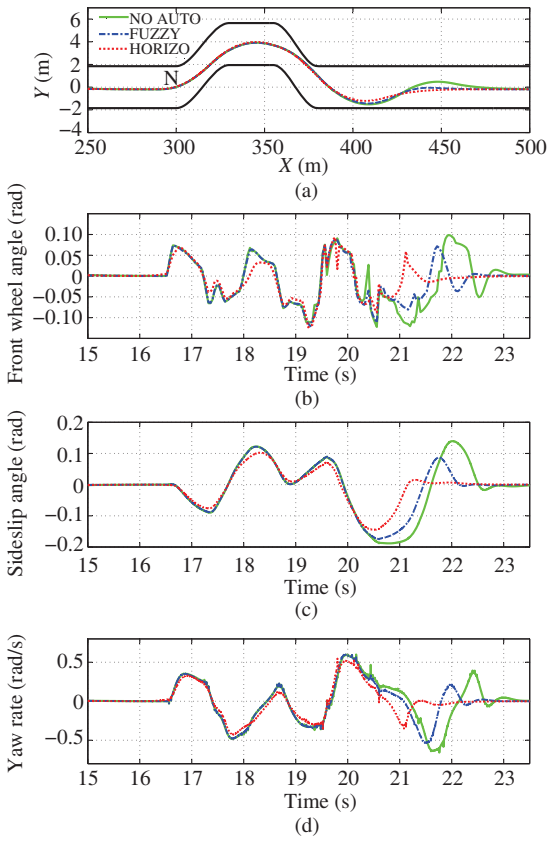

Figure 8 (Color online) Simulation results of high-risk double-lane change. (a) Vehicle trajectory; (b) front wheel angle; (c) sideslip angle; (d) yaw rate.

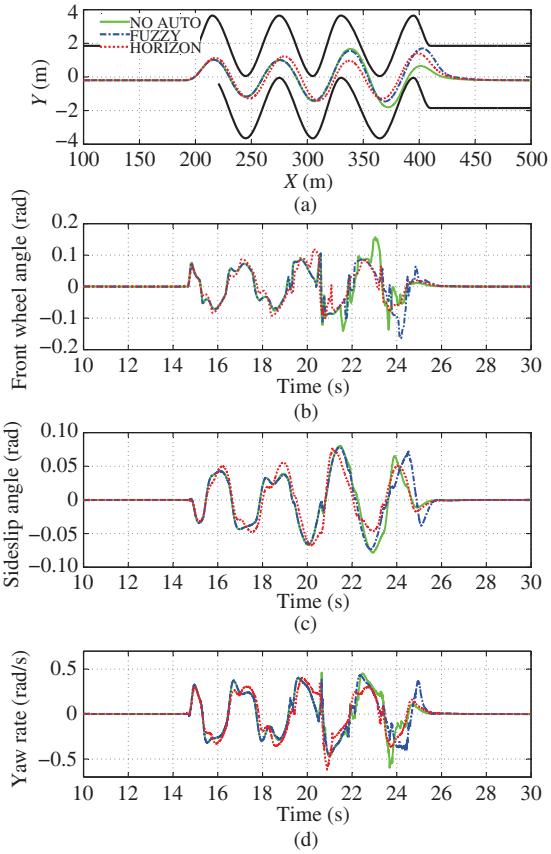

Figure 9 (Color online) Simulation results of high-risk slalom. (a) Vehicle trajectory; (b) front wheel angle; (c) sideslip angle; (d) yaw rate.

given in statistical form in Figure 10.

6.2.1 *High-risk double-lane change*

In test 2, the vehicle speed was set at 100 km/h, and the road friction coefficient was 0.55. The type D1 driver was selected to perform this driving test, in which the desired path was also a 0.2 m deviation from the centerline. As shown in Figure 8, the comparison of three schemes is given.

From the comparison of vehicle trajectories, similar results were obtained in the NO AUTO scheme and FUZZY scheme. A small difference in the trajectory of the FUZZY scheme exists, which converges faster than that of the NO AUTO scheme to the ideal trajectory after 400 m. Compared with the trajectory

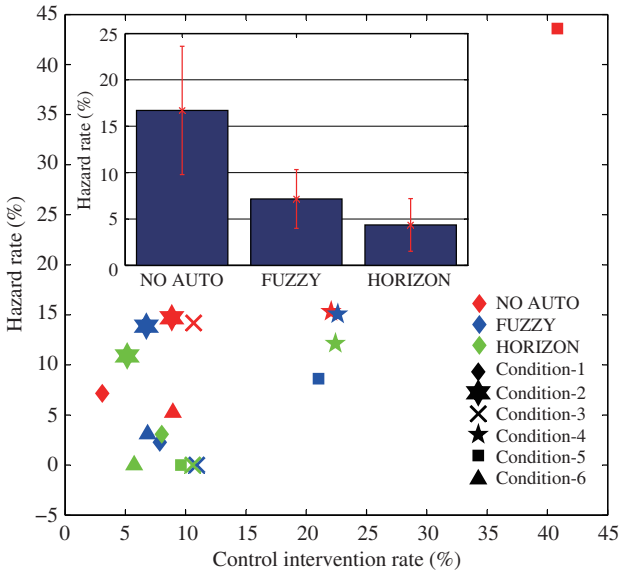

Figure 10 Comparison of high-risk scenario test results.

of the other two schemes, the trajectory of the HORIZON scheme has the fastest convergence speed. In the HORIZON scheme, the objective weight of tracking the ideal trajectory gradually increases in the predicted time domain, and tracking the driver's intention is considered as a secondary objective. Under such circumstances, the control outputs determined by the HORIZON scheme are more inclined to control the vehicle driving on the centerline of the road, leading to the fastest convergence speed to the road centerline. The first two schemes always follow the driver's intention as one of the main objectives, and the driver has more freedom with less interference from the controller. However, the sideslip angle and yaw rate of the first two schemes produce a greater oscillation after 400 m, which may make the vehicle more likely to lose stability. Benefiting from the higher intervention rate of the HORIZON scheme, the vehicle states can be maintained in a relatively stable range. The increased degree of driving freedom is at the expense of some stability. We can also draw this conclusion from the index of the hazard rate of the three schemes: the statistical results are 14.7095%, 13.8762%, and 10.8988%, respectively.

6.2.2 *High-risk slalom*

In test 1, the vehicle speed is 80 km/h, and the road friction coefficient is set to 0.75 in the slalom scenario. When driving in the slalom scenario, the driver was set to follow the line with a 0.2 m deviation from the centerline to imitate the real driver's misoperation on the actual road.

In Figure 9, the comparison simulation curves of trajectories, front wheel angle, sideslip angle and yaw rate are given. It is clear that all three schemes are available to make the vehicle remain within the road boundary when a misoperation of the human driver occurs. Due to the difference in objective explained in Subsection 6.2.1, the trajectory of the NO AUTO scheme is the most likely to collide with the road boundary compared with the two improved schemes, which can be observed from the vehicle trajectory between 380 and 430 m. The statistical hazard rates of the NO AUTO, FUZZY, and HORIZON schemes are 7.1596%, 2.2699%, and 3.0798%, respectively, demonstrating that the effective intervention of the FUZZY scheme and HORIZON scheme makes the vehicle safer if a dangerous situation occurs. In addition, the vehicle system obtains smoother control output, sideslip angle and yaw rate with the proper correction by the FUZZY and HORIZON schemes, as indicated by the results during 22–26 s in Figure 9. It is also illustrated that the FUZZY and HORIZON schemes can make the vehicle states convergence faster and smoother in dangerous scenarios.

Table 4 High-risk condition performance

Index	NO AUTO	FUZZY	HORIZON
Average hazard rate (%)	16.7056	7.1562	4.3529

6.2.3 *Evaluation and discussion*

In this part, all the simulation results of the six high-risk scenarios shown in Table 3 are presented in statistical form. The red, blue, and green colors represent the results of the NO AUTO, FUZZY, and HORIZON schemes, respectively. The simulation results of six high-risk scenarios shown in Table 3 are represented by symbols with different shapes, as shown in Figure 10.

In high-risk scenarios, safety attracts more attention, and the results of average hazard rates are shown in Table 4. In Table 4, the latter two schemes have a clear advantage over the NO AUTO scheme in ensuring vehicle safety because of their earlier time of intervention. A more detailed comparison is shown in Figure 10. In test 1, the NO AUTO scheme focused on following the driver's commands, failing to ensure a low hazard rate. In tests 2, 5, and 6, the latter two schemes guaranteed safety with a higher control intervention rate. In other words, they can interface drivers with assistance in early time when the driver's ability is insufficient. Moreover, the results of tests 5 and 6 in Figure 10 illustrate that the two improved schemes can significantly reduce the hazard rates in the scenarios that the driver has poor driving skills, demonstrating that the two improved schemes are robust to driver skill perturbations.

In general, the first scheme can provide more freedom for drivers at the expense of vehicle safety. And the latter two schemes benefit from the earlier intervention time to improve vehicle safety. Comparing the simulation results of six high-risk scenarios shown in Table 3, the latter two schemes have not significantly increased the control intervention rate in high-risk scenarios due to their smooth intervention characteristics, and even reduced the control intervention rate of the system in some scenarios. This shows that the latter two schemes are better than the first one in terms of security and subjective experience in high-risk scenarios. But the HORIZON scheme has a relatively higher control intervention rate compared with the other two schemes in low-risk scenarios, as shown in Figure 7. In low-risk scenarios, the latter two schemes are better than the first one in terms of security, and the HORIZON scheme will get relatively low subjective evaluation due to its relatively higher control intervention rate.

7 Conclusion

Three shared steering envelope control frameworks are designed to address the collaborative relationship between driver and shared steering controller in this paper. The first shared steering envelope control strategy can guarantee the driver's driving freedom to the greatest extent, while it has a risk of instability caused by improper operation by drivers. To remedy this shortcoming, two improved methods that consider the hazard risk and driver unreliability in the predictive time domain are proposed. The concrete manifestation of the improved methods is to redesign the objective function and the weight changing law of the objective function. Moreover, two novel evaluation indexes based on statistical principles are proposed to evaluate the performance of the shared steering envelope control. The simulation results under different scenarios show that the two proposed improved schemes can reduce the risk caused by improper driver operation at the expense of increasing the intervention rate, although it may have sacrificed minor subjective feelings of the driver. In addition, vehicle safety can be guaranteed with a lower control intervention rate if the prediction accuracy of driver's intent can be enhanced.

Acknowledgements This work was supported by National Natural Science Foundation of China (Grant Nos. U19A2069, 61790563, U1664263), Project of the Education Department of Jilin Province (Grant No. JJKH20190165KJ), and Project of Development and Reform Commission of Jilin Province (Grant No. 2019C036-5).

References

1 Veres S M, Molnar L, Lincoln N K, et al. Autonomous vehicle control systems — a review of decision making. Proc Inst Mech Eng Part I-J Syst Control Eng, 2011, 225: 155–195

2 Dixit S, Fallah S, Montanaro U, et al. Trajectory planning and tracking for autonomous overtaking: state-of-the-art and future prospects. Annu Rev Control, 2018, 45: 76–86
3 Hu C, Wang Z F, Taghavifar H, et al. MME-EKF-based path-tracking control of autonomous vehicles considering input saturation. IEEE Trans Veh Technol, 2019, 68: 5246–5259
4 Hu C, Chen Y M, Wang J M. Fuzzy observer-based transitional path-tracking control for autonomous vehicles. IEEE Trans Intell Transport Syst, 2020. doi: 10.1109/TITS.2020.2979431
5 van Brummelen J, O'Brien M, Gruyer D, et al. Autonomous vehicle perception: the technology of today and tomorrow. Transp Res Part C-Emerg Technol, 2018, 89: 384–406
6 Schoettle B, Sivak M. A Preliminary Analysis of Real-world Crashes Involving Self-driving Vehicles. The University of Michigan Transportation Research Institute Report UMTRI-2015-34. 2015
7 Schoettle B, Sivak M. Public Opinion About Self-driving Vehicles in China, India, Japan, the US, the UK, and Australia. The University of Michigan Transportation Research Institute Report UMTRI-2014-30. 2014
8 Mars F, Chevrel P. Modelling human control of steering for the design of advanced driver assistance systems. Annu Rev Control, 2017, 44: 292–302
9 Mars F, Deroo M, Hoc J M. Analysis of human-machine cooperation when driving with different degrees of haptic shared control. IEEE Trans Haptics, 2014, 7: 324–333
10 Kim J H, Song J B. Control logic for an electric power steering system using assist motor. Mechatronics, 2002, 12: 447–459
11 van der Wiel D W J, van Paassen M M, Mulder M, et al. Driver adaptation to driving speed and road width: exploring parameters for designing adaptive haptic shared control. In: Proceedings of IEEE International Conference on Systems, Man, and Cybernetics, Kowloon, 2015. 3060–3065
12 Abbink D A, Mulder M, van der Helm F C T, et al. Measuring neuromuscular control dynamics during car following with continuous haptic feedback. IEEE Trans Syst Man Cybern B, 2011, 41: 1239–1249
13 Abbink D A, Cleij D, Mulder M, et al. The importance of including knowledge of neuromuscular behaviour in haptic shared control. In: Proceedings of IEEE International Conference on Systems, Man, and Cybernetics (SMC), Seoul, 2012. 3350–3355
14 Iwano K, Raksincharoensak P, Nagai M. A study on shared control between the driver and an active steering control system in emergency obstacle avoidance situations. IFAC Proc Volumes, 2014, 47: 6338–6343
15 Boink R, van Paassen M M, Mulder M, et al. Understanding and reducing conflicts between driver and haptic shared control. In: Proceedings of IEEE International Conference on Systems, Man, and Cybernetics (SMC), San Diego, 2014. 1510–1515
16 Do M T, Man Z H, Zhang C S, et al. Robust sliding mode-based learning control for steer-by-wire systems in modern vehicles. IEEE Trans Veh Technol, 2014, 63: 580–590
17 Brandt T, Sattel T, Bohm M. Combining haptic human-machine interaction with predictive path planning for lane-keeping and collision avoidance systems. In: Proceedings of IEEE Intelligent Vehicles Symposium, Istanbul, 2007. 582–587
18 Mulder M, Abbink D A, Boer E R. Sharing control with haptics: seamless driver support from manual to automatic control. Hum Factors, 2012, 54: 786–798
19 Switkes J P, Rossetter E J, Coe I A, et al. Handwheel force feedback for lanekeeping assistance: combined dynamics and stability. J Dyn Syst Meas Control, 2006, 128: 532–542
20 Petermeijer S M, Abbink D A, de Winter J C F. Should drivers be operating within an automation-free bandwidth? Evaluating haptic steering support systems with different levels of authority. Hum Factors, 2015, 57: 5–20
21 Na X, Cole D J. Game-theoretic modeling of the steering interaction between a human driver and a vehicle collision avoidance controller. IEEE Trans Human-Mach Syst, 2015, 45: 25–38
22 Well K. Aircraft control laws for envelope protection. In: Proceedings of AIAA Guidance, Navigation, and Control Conference and Exhibit, Keystone, 2006. 258–267
23 Erlien S M, Funke J, Gerdes J C. Incorporating non-linear tire dynamics into a convex approach to shared steering control. In: Proceedings of American Control Conference, Portland, 2014. 3468–3473
24 Erlien S M, Fujita S, Gerdes J C. Shared steering control using safe envelopes for obstacle avoidance and vehicle stability. IEEE Trans Intell Transp Syst, 2016, 17: 441–451
25 Salvucci D D, Gray R. A two-point visual control model of steering. Perception, 2004, 33: 1233–1248
26 Nguyen A T, Sentouh C, Popieul J C. Driver-automation cooperative approach for shared steering control under multiple system constraints: design and experiments. IEEE Trans Ind Electron, 2017, 64: 3819–3830
27 Li R J, Li Y N, Li S B, et al. Driver-automation indirect shared control of highly automated vehicles with intention-aware authority transition. In: Proceedings of IEEE Intelligent Vehicles Symposium (IV), Redondo Beach, 2017. 26–32
28 Plöchl M, Edelmann J. Driver models in automobile dynamics application. Veh Syst Dyn, 2007, 45: 699–741
29 Biondi F, Alvarez I, Jeong K A. Human-vehicle cooperation in automated driving: a multidisciplinary review and appraisal. Int J Human-Comput Inter, 2019, 35: 932–946
30 Johns M, Mok B, Sirkin D, et al. Exploring shared control in automated driving. In: Proceedings of the 11th ACM/IEEE International Conference on Human-Robot Interaction (HRI), Christchurch, 2016. 91–98
31 Nishimura R, Wada T, Sugiyama S. Haptic shared control in steering operation based on cooperative status between a driver and a driver assistance system. J Human-Robot Inter, 2015, 4: 19–37
32 Tan D K, Chen W W, Wang H B, et al. Shared control for lane departure prevention based on the safe envelope of

steering wheel angle. Control Eng Practice, 2017, 64: 15–26
33 Saleh L, Chevrel P, Claveau F, et al. Shared steering control between a driver and an automation: stability in the presence of driver behavior uncertainty. IEEE Trans Intell Transp Syst, 2013, 14: 974–983
34 Wang W S, Xi J Q, Liu C, et al. Human-centered feed-forward control of a vehicle steering system based on a driver's path-following characteristics. IEEE Trans Intell Transp Syst, 2017, 18: 1440–1453
35 MacAdam C C. An optimal preview control for linear systems. J Dyn Syst Meas Control, 1980, 102: 188–190
36 Du H P, Zhang N, Dong G M. Stabilizing vehicle lateral dynamics with considerations of parameter uncertainties and control saturation through robust yaw control. IEEE Trans Veh Technol, 2010, 59: 2593–2597
37 Shen C, Shi Y, Buckham B. Integrated path planning and tracking control of an AUV: a unified receding horizon optimization approach. IEEE/ASME Trans Mechatron, 2017, 22: 1163–1173
38 Zhou L M, Jia L, Wang Y L. A robust integrated model predictive iterative learning control strategy for batch processes. Sci China Inf Sci, 2019, 62: 219202
39 Guo L L, Chen H, Gao B Z, et al. Energy management of HEVs based on velocity profile optimization. Sci China Inf Sci, 2019, 62: 089203
40 Felipe E, Navin F. Automobiles on horizontal curves: experiments and observations. Transp Res Record, 1998, 1628: 50–56
41 Bella F. Driver perception of roadside configurations on two-lane rural roads: effects on speed and lateral placement. Accid Anal Prev, 2013, 50: 251–262